Unified lowering decision of parametric thinning in the hypothesis test framework

Rabaa Youssef, Sylvie Sevestre-Ghalila

Unified lowering decision of parametric thinning in the hypothesis test framework

Rabaa Youssef*†
*COSIM Lab. in Sup'Com, University of Carthage
Cité Technologique des Communications, Tunisia
Email: rabaa.youssef@gmail.com

Sylvie Sevestre-Ghlalila†
CEA-LinkLab in Telnet Innovation Labs
Cité Technologique des Communications, Tunisia
Email: sylvie.sevestre@cea.fr

***Abstract*—Homotopic grayscale thinning leads to over-connected skeleton when applied on noisy images. To avoid this phenomenon, the parametric thinning relaxes the initial constraint by lowering low contrast crests, peaks and ends, according to a parameter related to the noise and contrast of the image and under the constraint of ascendant gray level processing. Even if the statistical control of this parameter leads to a local adjustment and to a standardization of the thinning parameter, this method still produces spurious branches. In fact, the lowering criterion for peak and end notions becomes unadapted while the image dynamic changes during the thinning process. To avoid this phenomenon, we propose to revise and unify these lowering criteria. Consequently, we update the statistical test design by taking into account the gray level of the treated pixels to better fit to lowerable pixels definition. Results of our contribution are compared to the initial parametric thinning.**

Keywords: Thinning, mathematical morphology, homotopy, hypothesis test.

Introduction

Skeletonization is an image transformation that aims to represent objects by their medial axis lines while preserving image topology. It results in a one-pixel thin line called skeleton. The main approaches of skeletonization are based either on mathematical morphology or on differential geometry. Despite the medial axis accuracy of the latter detectors [1], [2], the complex setting of their parameters and especially their inability to preserve the connectedness of objects (homotopy of skeleton) limits their applicability to regular object lines with few junctions. Concerning the morphology based skeletonization category, a focus on the thinning methodologies is noticed for their topology preservation property. Therefore, the homotopic thinning has been widely investigated in the early 90's by [3], [4], pointing out the role of this category of methods in feature extraction as an important step of pattern recognition applications. One can cite their usefulness for character recognition application [5], [6], [7] in binary context and in the fields of road extraction [8], [9], biomedical imaging [10] and biometrics [11], [12] in grayscale one.

As it was initially implemented for binary images, the thinning was extended to grayscale images by [13], [14], [15] through the use of the cross-sectional topology. Instead of successively peeling border pixels until reaching object medial axis, grayscale thinning consists in sequential lowering of gray values starting from background pixels until reaching object highest crest lines representing the skeleton. The ensuing improvement of the grayscale thinning was the consideration of noisy image context. To do so, the authors of [16] propose to relax the topology preservation constraint by involving in the lowering condition topological notions of peak, end and crest pixels which are controlled by a parameter denoted λ. Therefore, the efficiency of the lowering requires an accurate setting of the parameter λ which is so far, manually set.

In [17], the authors showed that the lowering step of each thinning topological notion can be assimilated to a statistical hypothesis test based on order statistics. Thanks to this framework, they replaced the manually set parameter by a standardized confidence levels of the used statistical tests for the lowering decision in the three configurations. The introduction of statistical tests allows good control of the lowering of the crests without sufficiently removing insignificant peaks and ends. In fact, these pixels are mostly treated at late stages of the thinning. This induces large changes in the dynamic of the image making the lowering decision not adapted to the current skeletonized image.

The present work aims to propose a revision of the lowering criterion for *peak* and *endpoint* decisions. This new scheme permits us not only to eliminate more efficiently these pixels, but also to implement a common statistical strategy for the lowering decision of the three thinning notions. In addition, we revise the statistical test by taking into account the cross section information in the test design.

In a first section, we present the parametric thinning framework. In the second, we unify the lowering criterion of the three topological notions by updating the lowering criterion for peak and end pixels. The third section is devoted to the revision of statistical control of the thinning parameter proposed by [17]. We end up presenting results on synthetic images to assess our contribution.

I. Parametric thinning framework

The grayscale thinning framework is extended from the binary thinning one by using the cross-sectional topology introduced in [13], [14], [15]. The principle of grayscale thinning is to identify lowerable pixels, iteratively lowered by setting them to the gray value of their respective closest dark neighbor. The cross-section binarizes the 8-nearest neighbors of each pixel x ($\mathcal{N}_8(x)$) and splits them into two subsets. By denoting $I(x)$ the gray intensity of pixel x, the two subsets are defined as follows:

- The set of darker 8-neighbors of x $\mathcal{N}_8^<(x) = \{y \in \mathcal{N}_8(x), I(y) < I(x)\}$ which is involved in the lowering step of thinning algorithm,
- The set of higher 8-neighbors of x $\mathcal{N}_8^\geq(x) = \{y \in \mathcal{N}_8(x), I(y) \geq I(x)\}$. The spatial configuration of this set is used to decide if x is *lowerable*.

For the first grayscale thinning algorithm, J. Serra [13] defined a *lowerable* pixel x as *simple* for the cross-section as explained hereafter:

Definition 1: A *simple* pixel x verifies the following two conditions:

(i) At least one of the 4-nearest neighbors of a pixel x belongs to $\mathcal{N}_8^<(x)$,
(ii) $\mathcal{N}_8^\geq(x)$ forms a unique 8-connected component.

The condition (i) states simply that x is a border object and condition (ii) that removing x doesn't change the object connectedness. In order to prohibit the lowering of pixels in branche's extremity, the *endpoint* pixels are blocked in gray thinning as proposed by A. Rosenfeld in [18] for binary images. G. Bertrand [19] and M. Couprie [16] defined the *endpoint* notion in grayscale image as follows:

Definition 2: An object pixel x is an *endpoint* if it has only one 8-neighbor belonging to the foreground: $|\mathcal{N}_8^\geq(x)| = 1$.

Therefore, the *lowerable* pixels are *simple* pixels that are not *endpoint*. However, this definition of *lowerable* does not take into account isolated pixels. To treat these pixels, the last topological notion of *peak* is added to the *lowerable* pixels set of classical thinning. It was defined as follows [19], [16]:

Definition 3: An object pixel x is *peak* if it has no 8-neighbor belonging to the foreground: $|\mathcal{N}_8^\geq(x)| = 0$.

The Algorithm 1 details this thinning process.

Algorithm 1 Thinning algorithm for grayscale image

Require: $I(x)$ grayscale value of pixel x in image I
repeat
  Compose the list $\mathfrak{L}$ of *lowerable* pixels in I
  for Pixel x in $\mathfrak{L}$ **do**
    if x is still *lowerable* at this step **then**
      $I(x) \leftarrow max\{I(y), y \in \mathcal{N}_8^<(x)\}$
    end if
  end for
until $\mathfrak{L}$ is empty

The ensuing improvement of the classical thinning framework is the consideration of noise in grayscale images. In fact, the thinning of noisy images generates non-significant crests, extremities and isolated pixels and results in over-connected and inexploitable skeletons.

Consequently, the authors of [16] relaxed the strong constraint of preserving connectedness when a local contrast is below a global parameter λ. The main idea of this method called λ-Skeleton is to revise *lowerable* pixels set by:

1) adding the topological configuration of *crest* pixels,
2) introducing λ-lowerable pixels as insignificant *peaks*, *crests* and *endpoints*. They are all controlled by the global parameter λ and involved in the lowering process in parallel to *simple* pixels still belonging to *lowerable* set.

Related to this idea, definitions of λ-*crest*, λ-*end* and λ-*peak* are detailed in the following.

Definition 4: Pixel x is λ-*crest* if it fulfills the following two conditions:

(i) At least 2 connected components ($\mathcal{K} \geq 2$) in $\mathcal{N}_8^<(x)$ are 4-connected and 4-adjacent to x;
(ii) For these $\mathcal{K}$ connected components, named C_k ($k = 1, .., \mathcal{K}$), at least $(\mathcal{K} - 1)$ are at minor distance from I(x):

$$d_1(x, C_k) = (\, I(x) - \min\{I(C_k)\}\,) \leq \lambda.$$

Condition (i) in the λ-*crest* Definition 4, states that pixel x lies locally on a crest surrounded by $\mathcal{K}$ darker components. Condition (ii) states that no more than one darker component is at a distance exceeding λ, thus that the crest pixel may be assimilated to the local background represented by the other $(\mathcal{K} - 1)$ dark components. It is worth noting that 4-connectedness and 4-adjacency conditions limit $\mathcal{K}$ to $2 \leq \mathcal{K} \leq 4$, as illustrated in Figure 1.

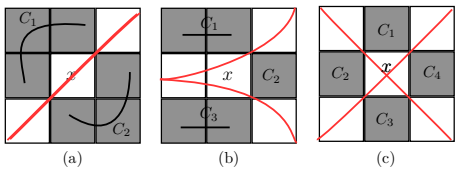

Fig. 1. In each one of the configurations, x is λ-*crest* for $\mathcal{K} = 2$ (left), $\mathcal{K} = 3$ (middle) and $\mathcal{K} = 4$ (right).

Definition 5: Pixel x is λ-*end* (resp. λ-*peak*) if x is *end* (resp. *peak*) pixel and:

$$d_2(x, C) = (\, I(x) - \max\{I(C)\}\,) \leq \lambda$$

where C is the unique 8-connected component of the lower 8-neighborhood of the pixel x $\mathcal{N}_8^<(x)$.

These λ-dependant configurations are merged in the single λ-*lowerable* notion of definition 6.

Definition 6: Pixel x is λ-*lowerable* if it satisfies one of the following conditions:

(i) x is λ-*crest* (ii) x is λ-*end* (iii) x is λ-*peak*.

An overall graph of lowering cases for the λ-thinning is presented in Figure 2, where we differentiate λ-dependant configurations (λ-*lowerable*) from topology preserving *simple* pixels (*lowerable*). As mentioned in Algorithm 2,

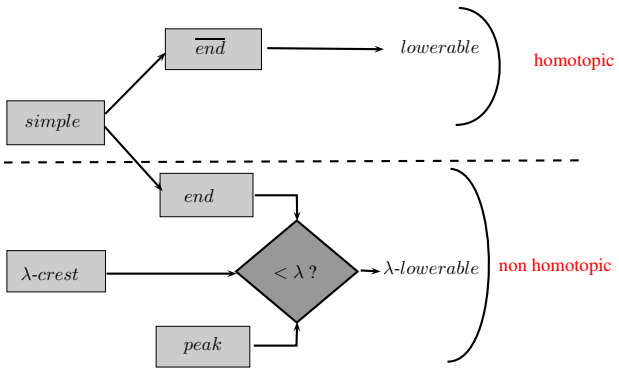

Fig. 2. Description of λ-*lowerable* pixel [17]: $\overline{end}$ denotes a *non-endpoint* pixel.

the λ-Skeleton treats pixels in an ascendant order of intensity to avoid trespassing object crest lines and disconnecting them. In the appendix of [16], the authors explain that a sorting step on the list of λ-*lowerable* pixels needs to be performed before thinning so that object crest disconnections are avoided as much as possible. In fact, low crests are located not only in the background, but also in the foreground. Their processing in the first iterations may reduce their local contrast to neighbors and melt them with the insignificant crests in the upcoming iterations.

Algorithm 2 $\lambda-$*thinning* algorithm for grayscale image

Require: $I(x)$ grayscale value of pixel x in image I

repeat
  Compose the list $\mathfrak{L}$ of λ-*lowerable* or *lowerable* pixels in I
  Sort the list $\mathfrak{L}$ in an increasing order of intensity
  Extract from $\mathfrak{L}$ the pixels with minimal values to form $\mathfrak{L}'$
  for Pixel x in $\mathfrak{L}'$ **do**
    if x is still λ-*lowerable* or *lowerable* at this step **then**
      $I(x) \leftarrow max\{I(y), y \in \mathcal{N}_8^{\leq}(x)\}$
    end if
  end for
until $\mathfrak{L}$ is empty

Two main changes are noted between the classic gray thinning and the parametric thinning of Algorithm 2. The first is the use of homotopy changing configurations in the lowering process so that noisy pixels are filtered. The second is the ascendant treatment of the image gray levels to limit object disconnection induced by the treatment of non-homotopic configurations.

II. Update of thinning strategy for the lowering of peak and endpoint

According to Definitions 4 and 5, we note a difference in the choice of distance between $I(x)$ and the darker component of x neighborhood. The Definition 4 (of λ-*crest*) is based on the distance d_1 between the gray level $I(x)$ and the darkest gray level of the neighboring component C, while the brightest level in C is chosen based on the distance d_2 between C and the central pixel in case of λ-*end* and λ-*peak* configurations.
The latter choice permits to better adapt the lowering decision to the gray ordered treatment of the parametric thinning procedure that mostly lowers *peaks* and *endpoints* at the final iterations. This is due to the fact that *peaks* and *endpoints* have higher gray values than crest lines as shown in Figure 3. At the late stages of the processing, the distance d_1 used for λ-*crest* is no longer adapted to λ-*end* and λ-*peak* configurations, since the darker neighbors used for this distance will inevitably be treated first. This results in a change of the low neighborhood gray values and in an unsuitable increase of the distance d_1. Hence, the lowering of λ-*end* and λ-*peak* configurations may rarely be verified. Therefore, the choice of d_2 of Definition 5 that compares the tested pixel to its highest darker neighbor might limit the impact of previous iterations on the local gray level dynamic. This close dark neighbor is less likely to be affected by previous peelings and thus d_2 appears to be more adapted to λ-*end* and λ-*peak*. Since we choose not to change the treatment

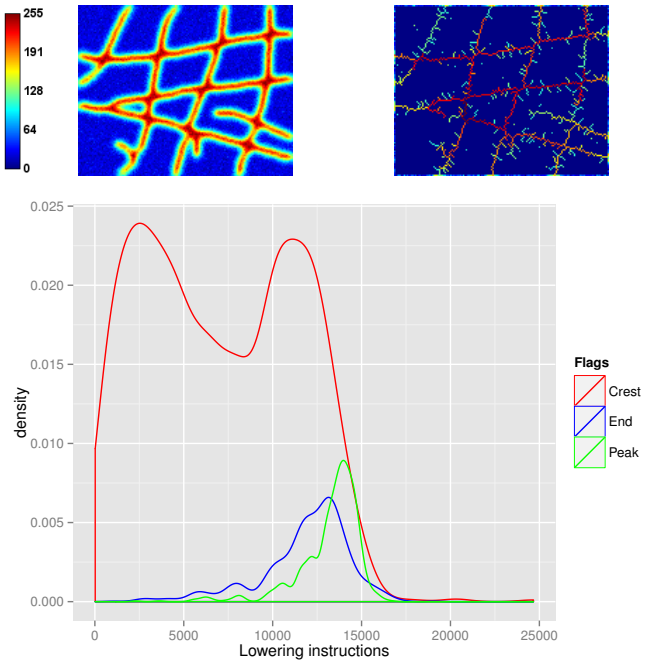

Fig. 3. First line: λ-Skeleton result on synthetic image with white Gaussian noise of $\sigma_{noise} = 5$ in jet color map. Second line: Order treatment of λ-dependent configurations through successive lowering instructions for synthetic image.

order of the parametric thinning, we have to assume the change of the image dynamic during the thinning process. To overcome the dynamic change issue for the upcoming peelings, we first propose to use the initial image I_0 gray levels in order to decide to lower λ-peak and λ-end pixels. Second, we estimate the height of *peak* and *endpoint* from their respective local dark neighborhood by using a distance inspired from the λ-crest Definition 4. Consequently, the revised definition of λ-peak and λ-end is:

Definition 7: Pixel x is λ-peak (resp. λ-end) if x is *peak* (resp. *end*) according to the $\mathcal{N}_8^{\leq}(x)$ configuration and:

$$d(x, C) = (I_0(x) - min(I_0(C))) \leq \lambda \quad (1)$$

where C is the unique 8-connected component in $\mathcal{N}_8^{\leq}(x)$ obtained from the current image I and $I_0(C)$ is composed of initial gray values of C.
This revision unifies the criterion for all λ-dependent configurations. In this new context, we update in Section III the hypothesis test framework for the lowering decision in order to set the parameter λ to an appropriate threshold.

III. Hypothesis test of unified lowering decision

Statistical tests to manage the lowering decision were presented in [17]. Based on the unique significance level α, the thinning setting became locally adjusted and thus less user dependent than initial globally and manually chosen λ. In the unified context of the proposed lowering, we update in this section the unique statistical test by taking into account the gray level of the treated pixels to better fit the definitions of λ-*lowerable* pixels. The first subsection develops the statistical test related to *peak* and *endpoint* lowering decision. The next subsection details the transposition of this test in the case of λ-crest configuration.

A. Hypothesis test for the lowering of peak and endpoint

According to the criterion of equation 1 in Definition 7, deciding that x is a lowerable peak (resp. end) is tantamount to saying that x belongs to the unique connected component C consisting in $\mathcal{N}_8^{\leq}(x)$. Thereby, $I_0(x)$ is seen as a further observation of the sample composed of initial gray levels of the connected component C, where $n = |C \cup \{x\}|$ is the size of the sample $X_C = (X_1, \ldots, X_n)$ and $I_0(x)$ is its maximum value.
As stated in [17], this criterion can be used as a decision rule of a statistical test where the null hypothesis (H_0) refers to the fact that the central pixel x is a λ-lowerable *peak* (resp. *endpoint*) and its alternative hypothesis (H_1) meaning that x is a significant *peak* (resp. *endpoint*) and has to be maintained. The authors transpose the lowering criterion of *peak* and *endpoint* to reach a test statistic designed as the range one. Therefore, by assuming that each variable X_i of the sample X_C under the null hypothesis (H_0) is $X_i \sim \mathcal{N}(\mu, \sigma)$, $\forall i = 1 \ldots n$ and for a given test level α, the authors accept H_1 when:

$$X_{(n)} - X_{(1)} > \lambda = \sigma\tau_n(\alpha)$$
$$\text{with } X_{(1)} = \min_{i=1\ldots n} X_i \text{ and } X_{(n)} = \max_{i=1\ldots n} X_i$$

and where $\tau_n(\alpha)$ is the α quantile of the range distribution of a Gaussian sample $\mathcal{N}(0, 1)$. So, the threshold value λ can be evaluated directly from the fixed significance level α and the size n of the connected component C ($n = 9$ for *peak* configuration and $n = 8$ for *endpoint* configuration).

One can notice that the pixel set C is obtained considering the knowledge of the gray value of the examined pixel x. Consequently, one can accept H_1 when:

$$X_{(n)} - X_{(1)} > \lambda \text{ knowing } X_{(n)} = I_0(x)$$

Noting $X_i = \mu + \sigma \cdot Y_i$ with $Y_i \sim \mathcal{N}(0, 1)$, $Y_{(1)} = \min_{i \in C} Y_i$ and $Y_{(n)} = \max_{i \in C} Y_i$ and for a test level α, we can state that:

$$P_{H_0}\left(X_{(1)} < I_0(x) - \lambda \mid X_{(n)} = I_0(x)\right) = \alpha \Leftrightarrow$$
$$P_{H_0}\left(Y_{(1)} < \frac{I_0(x) - \mu - \lambda}{\sigma} | Y_{(n)} = \frac{I_0(x) - \mu}{\sigma}\right) = \alpha \quad (2)$$

Consequently, the test statistic used according to Definition 7 of lowerable peaks or ends is the minimum statistic of the corresponding sample X_C under the knowledge of its maximum gray level ($I_0(x)$). By using the well-known cumulative distribution of such i.i.d sample [20], Equation 2 becomes:

$$1 - \left(1 - \frac{F(1/\sigma[I_0(x) - \mu - \lambda])}{F(1/\sigma[I_0(x) - \mu])}\right)^{n-1} = \alpha$$

where F is the cumulative distribution function of $\mathcal{N}(0, 1)$. Therefore, we have:

$$(1 - \sqrt[n-1]{1-\alpha})F(1/\sigma[I_0(x) - \mu]) = F(1/\sigma[I_0(x) - \mu - \lambda])$$

Let us denote $\tau_n(\alpha) = 1/\sigma[I_0(x) - \mu - \lambda]$. Therefore, $\tau_n(\alpha)$ is the quantile of $\mathcal{N}(0, 1)$ and can be expressed as follows:

$$\tau_n(\alpha) = F^{-1}_{\mathcal{N}(0,1)}\left((1 - \sqrt[n-1]{1-\alpha})F_{\mathcal{N}(0,1)}(1/\sigma[I_0(x) - \mu])\right) \quad (3)$$

which leads to the determination of λ such as:

$$\lambda = I_0(x) - \mu - \sigma\tau_n(\alpha). \quad (4)$$

Finally, according to the expression of λ in Equation 4, the criterion of Equation 1 that permits to lower insignificant peaks and ends when knowing $X_{(n)} = I_0(x)$ becomes:

$$X_{(1)} \geq \mu + \sigma\tau_n(\alpha) \quad (5)$$

B. Hypothesis test of crest lowering decision

According to Definition 4, the criterion that permits to lower a crest pixel x is that among his $\mathcal{K}$ darker neighboring components, named C_k for $k = 1 \dots \mathcal{K}$, at least $(\mathcal{K} - 1)$ verify:

$$I(x) - \min\{I(C_k)\} \leq \lambda \tag{6}$$

In the case of lowerable crests, $\mathcal{K}$ unitary statistical tests can be designed similarly to that presented for *peak* and *endpoint*. Therefore, the previously designed statistical test is applied to each of the $\mathcal{K}$ connected components using current image gray values. Thus for C_k connected components, the determination of λ becomes:

$$\lambda = I(x) - \mu - \sigma \cdot \tau_n(\alpha) \tag{7}$$

where $n = |C_k|$ and μ is the mean of the iid sample X_{C_k}.

The quantile τ_n of Equation 3 is also calculated using the current image gray values:

$$\tau_n(\alpha) = F^{-1}_{\mathcal{N}(0,1)}\left((1 - \sqrt[n-1]{1-\alpha}) \cdot F_{\mathcal{N}(0,1)}(1/\sigma[I(x) - \mu])\right) \tag{8}$$

where $\alpha \in [0, 1]$.

In accordance with the Definition 4, a λ-crest pixel is lowered if at least 2 connected components of the dark neighborhood satisfy the Equation 6.

Finally, and in order to calculate λ at each pixel x, we need to estimate μ and σ. Firstly, the standard deviation σ of the sample could be assimilated to the image noise standard deviation. Under the assumption of a stationary Gaussian noise, we can consider that noise standard deviation σ is constant over the entire image and could be empirically estimated for real images. Secondly, μ is the mean of the sample, and varies depending on X_C. The parameter μ is estimated empirically on each X_C by $\overline{X}_C = 1/n \cdot \sum_{i=1}^{n} X_i$. We calculate the mean on the initial image for *peak* and *endpoint* configurations and on the current image gray levels for λ-crest ones.

In the next, the proposed method is called α-Skeleton since it relies essentially on the choice of the confidence level.

IV. Results

We propose to compare our contribution denoted α-Skeleton to the initial method λ-Skeleton of [16] at our disposal on the author laboratory website. To do so, we present in a first section the synthetic images and the measures used for this assessment. In the next subsection, we detail the parameters setting of both methods. Finally, we implement the evaluation by assessing methods robustness to noise and discuss the results.

A. Data and measure for the assessment

In order to test the ability of skeletonization methods to preserve connectivity and free extremities, we generate the network image I_{N} of Figure 4 from the reference skeleton S^*_{N}. The gray network is obtained after a binary dilation with a disk of radius $\rho = 1$ followed by an averaging filter with kernel of radius $r_f = 7$.

We use a uniform background gray level (set to 25 in Figure 4) to avoid any truncation of the added noise values on the original images when simulating distortions.

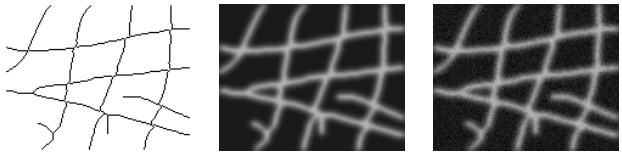

S^*_{N} $\quad D = 46$ $\quad I_{\mathrm{N}}$ $(\sigma = 8.5)$

Fig. 4. Left: binary reference skeleton S^*_{N}. Middle: smooth grayscale images with an average contrast D between foreground and background. Right: Image affected by an additive Gaussian noise on the grayscale images of second line with I_{N}: 150×121.

A set of $N = 20$ synthetic images is produced by varying the standard-deviation σ of the additive white Gaussian noise n_σ within $[2.5, 12.5]$ by a step of 0.5. From these images, the real skeletons S are extracted with the two retained methods.

In the following, we define the measures of Cp, Cr, OCC and E used in this assessment.

The preservation of topological characteristics of an object is objectively measured by the following normalized differences OCC and E:

$$OCC = \frac{\text{Nb OCC}(S^*) - \text{Nb OCC}(S)}{\text{Nb OCC}(S^*)},$$

$$E = \frac{\text{Nb E}(S^*) - \text{Nb E}(S)}{\text{Nb E}(S^*)}$$

where Nb OCC is the number of object components and, Nb E is number of skeleton ends. The ideal values for OCC and E are around zero, negative ratios correspond to the emergence of extra and insignificant information while positive values correspond to missing information in the real skeleton. These measures may diverge, as in the case where the number of ends of S is much larger than that of S^*. Hence, large values (respectively small) are clipped to 5 (respectively -5).

Besides, we calculate the completeness Cp and correctness Cr measures of the *buffer zone* method [21], [22] generally used to evaluate the geometrical accuracy of the real skeleton compared to the reference one.

B. Implementation of the evaluation

Both methods require the setting of a parameter. Indeed, for α-Skeleton, we need to choose the confidence level of the test which is classically set to $\alpha = 5.10^{-2}$. Concerning λ-Skeleton method, we propose to set its global parameter λ using the mean value of the lowering threshold $\tau_n(\alpha)$ (as calculated by Equations 8 and 3) and the noise standard deviation according to the formula: $\lambda = \text{mean}\tau_n(\alpha).\sigma_{noise}$.

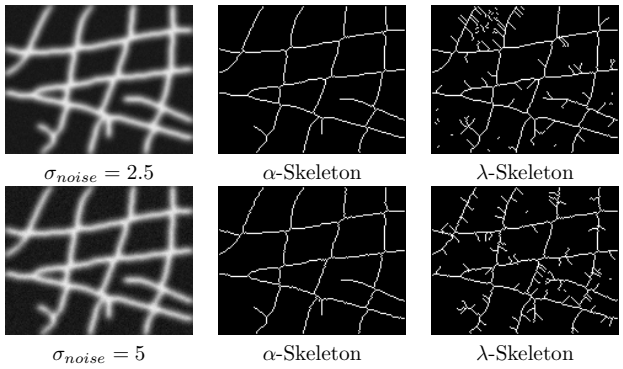

Fig. 5. Thinning results on the network synthetic image. White gaussian noise applied with $\sigma_{noise} = 2.5$ and $\sigma_{noise} = 5.1$.

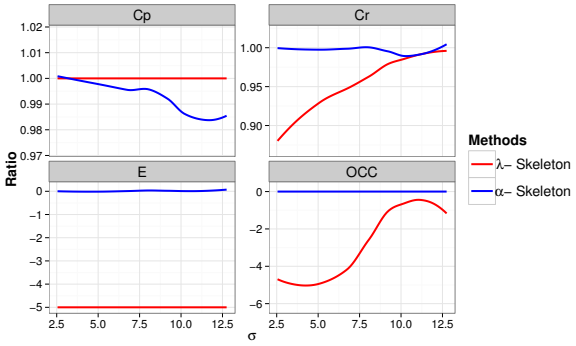

Fig. 6. Evaluation graphs for the synthetic image using Cp, C_r, OCC and E measures. Gaussian noise varying in $[2.5, 12.5]$.

Figure 5 and 6 shows the stability of α-Skeleton compared to λ-Skeleton especially regarding the elimination of spurious branches.

V. Conclusion

Grayscale thinning is a powerful morphological tool used to represent the essential information of an object by successively lowering image gray levels until reaching central crest lines. Its sensitivity to noise in grayscale images implied the inclusion of noise related configurations in the lowering process. These lowerable notions need to be controlled to avoid disconnections. Due to the permanent change of the image intensities distribution during the thinning process, a control of the lowering decision is required by considering initial image gray values in order to efficiently eliminate isolated peaks and spurious branches. This revision of the lowering criteria enables us to unify the decision of all the concerned configurations. In addition, the design of hypothesis test for the lowering decision conditionally controlled by the gray level of each pixel enables us to calculate locally the adapted threshold λ and maintain the significantly contrasted object branches. The evaluation results exhibits the ability of α-Skeleton to maintain object connectedness and preserve only significant branches when applying white Gaussian noise on synthetic images.

References

[1] C. Steger, "An unbiased detector of curvilinear structures." *IEEE Trans. Pattern Anal. Mach. Intell.*, vol. 20, no. 2, pp. 113–125, 1998.

[2] I. Laptev, H. Mayer, T. Lindeberg, W. Eckstein, C. Steger, and A. Baumgartner, "Automatic extraction of roads from aerial images based on scale space and snakes," *Machine Vision and Applications*, vol. 12, no. 1, pp. 23–31, 2000.

[3] L. Lam, S.-W. Lee, and C. Y. Suen, "Thinning methodologies - a comprehensive survey," *IEEE Trans. Pattern Anal. Mach. Intell.*, vol. 14, no. 9, pp. 869–885, 1992.

[4] B. Jang and R. Chin, "One-pass parallel thinning: analysis, properties, and quantitative evaluation," *IEEE Trans. Pattern Anal. Mach. Intell.*, vol. 14, no. 11, pp. 1129–1140, 1992.

[5] L. Lam and C. Suen, "Evaluation of thinning algorithms from an ocr viewpoint," in *Document Analysis and Recognition, 1993., Proceedings of the Second International Conference on*, 1993, pp. 287–290.

[6] Y.-S. Chen and Y.-T. YU, "Thinning approach for noisy digital patterns," *Pattern Recognition*, vol. 29, no. 11, pp. 1847 – 1862, 1996.

[7] S. Wshah, Z. Shi, and V. Govindaraju, "Segmentation of arabic handwriting based on both contour and skeleton segmentation." in *ICDAR*. IEEE Computer Society, 2009, pp. 793–797.

[8] J. Mena and J. Malpica, "An automatic method for road extraction in rural and semi-urban areas starting from high resolution satellite imagery," *Pattern Recognition Letters*, vol. 26, no. 9, pp. 1201 – 1220, 2005.

[9] G. Lisini, C. Tison, F. Tupin, and P. Gamba, "Feature fusion to improve road network extraction in high-resolution sar images," *Geoscience and Remote Sensing Letters, IEEE*, vol. 3, no. 2, pp. 217–221, 2006.

[10] P. Yim, P. Choyke, and R. Summers, "Gray-scale skeletonization of small vessels in magnetic resonance angiography," *Medical Imaging, IEEE Transactions on*, vol. 19, no. 6, pp. 568–576, 2000.

[11] P. M. Patil, S. R. Suralkar, and F. B. Sheikh, "Rotation invariant thinning algorithm to detect ridge bifurcations for fingerprint identification." in *ICTAI*. IEEE Computer Society, 2006, pp. 634–641.

[12] F. Zhao and X. Tang, "Preprocessing and postprocessing for skeleton-based fingerprint minutiae extraction," *Pattern Recognition*, vol. 40, no. 4, pp. 1270 – 1281, 2007.

[13] J. Serra, *Image Analysis and Mathematical Morphology*. London: Academic Press, 1982.

[14] S. Beucher and J. Serra, "Shapes and patterns of microstructures considered as grey-tone functions," in *3rd European Symposium on Stereology, Ljubljana*, 1981.

[15] C. Ronse, "A topological characterization of thinning," *Theoretical Computer Science*, vol. 43, no. 0, pp. 31 – 41, 1986.

[16] F. N. B. e. G. B. M. Couprie, "Grayscale image processing using topological operators," in *SPIE Vision Geometry VIII.*, vol. 3811, 1999, pp. 261–272.

[17] R. Youssef, S. Sevestre-Ghalilai, and A. Ricordeau, "Statitical control of thinning algorithm with implementation based on hierarchical queues," in *Soft Computing and Pattern Recognition, 2014 6th International Conference of*, Aug 2014, pp. 365–370.

[18] Rosenfeld, "Connectivity in digital pictures," *Journal of the ACM*, 1970.

[19] G. Bertrand, J. christophe Everat, and M. Couprie, "Image segmentation through operators based upon topology," 1997.

[20] M. Cottrel, V. Genon-Catalot, and G. RUGET, *Exercices de probabilités avec rappel de cours*, ser. Dia. Paris: Belin, 1980, maîtrises de mathématiques pures et appliquées. Ecole d'ingénieurs.

[21] C. Heipke, H. Mayer, C. Wiedemann, and O. Jamet, "Evaluation of automatic road extraction," in *In: International Archives of Photogrammetry and Remote Sensing*, 1997, pp. 47–56.

[22] X. Guo, D. Dean, S. Denman, C. Fookes, and S. Sridharan, "Evaluating automatic road detection across a large aerial imagery collection," in *Digital Image Computing Techniques and Applications (DICTA), 2011 International Conference on*, Dec 2011, pp. 140–145.